A robustness approach to study metastable behaviours in a lattice-gas model of swarming

Olivier Bouré, Nazim Fatès, Vincent Chevrier

A robustness approach to study metastable behaviours in a lattice-gas model of swarming

Olivier Bouré, Nazim Fatès, Vincent Chevrier
LORIA – Inria nancy Grand-Est – Université de Lorraine

Abstract

Research in biology is increasingly interested in discrete dynamical systems to simulate natural phenomena with simple models. But how to take into account their robustness? We illustrate this issue by considering the behaviour of a lattice-gas model with an alignment-favouring interaction rule. This model, which has been shown to display a phase transition between an ordered and a disordered phase, follows ergodic dynamics. We present a method based on the study of stability and robustness, and show that the organised phase may result in several different behaviours. We then observe that behaviours are influenced asymptotically by the definition of the cellular lattice.

Keywords: Swarming behaviour ; lattice-gas cellular automata ; phase transitions ; robustness ; discretisation effects ; resonance effects

Introduction

Research on natural systems has thrived in the past years with the use of dynamical systems to simulate their behaviour, mainly through two types of opposing modelisation approaches. On the one hand, realistic approaches intend to copy the structure of the original system in order to faithfully reproduce its behaviour, often at the expense of a large parametrical space and a high computational cost. On the other hand, simplistic approaches, such as Turing's 1952 reaction-diffusion model [1], consider that complex behaviours can emerge from simple mathematical models. Indeed, their simulation allows a quick exploration of the space of individual behaviours, and provide good statistical data by repeating experiments. Also, reproducing complex phenomena with simple models may help us identify more precisely the role of each component of the model and explicit the necessary conditions for the emergence of the studied phenomenon (see *e.g.* [2] and ref. therein).

However, the use of simple models inevitably alters the way entities interact with each other and could affect the system's behaviour by introducing novel phenomena. Also, the implementation process, which consists of translating a model into a runnable simulation, can induce biases in the system's behaviour

by arbitrarily fixing specific components of the model (*e.g.* [3]). Thus, when studying the behaviour of a model through simulation, one may want to distinguish the aspects of the behaviour emerging from the interaction of local entities, from those induced by the simulation context. We propose to tackle this question in the light of the robustness of the model, that is, "the degree to which [the behaviour] is insensitive to effects that are not considered in the design" [4]. An intuitive method for detecting such effects consists in studying extensively the dynamics of the system under different simulation conditions and search for modifications of the behaviour (*e.g.* [5, 6]).

A particularly adapted subject of study of simple models simulating complex phenomena is *collective motion*, that is, the coordinated movement of entities with local interaction, for it has been extensively studied as an emergent behaviour in numerous natural systems [7, 8]. Using a wide range of models from self-propelled particles [9] to cellular automata [10], it was possible to study real-life phenomena in order to understand their mechanisms [11, 12, 13]. In other contexts, the same models have also been used as a simulation tool for human crowds [14, 15], as well as an algorithm of spatial computing [16, 17]. The dissociation of a model from its original context suggests changes in the simulation conditions and hypotheses, which might affect the behaviour and exhibit previously unobserved phenomena. This means our method consists in exploring the whole range of behaviours of the considered model, especially beyond the original context relevant to this model.

The *Vicsek model* was introduced in 1995 as a model of "self-propelled particles" moving at constant speed in a continuous space [18]. Assuming a stochastic direction-averaging rule, with a single parameter modulating the alignment behaviour from random to deterministic orientation, Viscek *et al.* observed the *swarm instability*, that is, a phase transition that separates chaotic, random motion from complete alignment of the particles. Simplifying the local rule opened the way to diverse studies: Peruani *et al.* predicted a continuous phase transition via a mean-field approach for self-propelled particles [19] and exhibited differences of behaviour for polar and apolar local rules [9]. Similarly, Chaté *et al.* investigated the influence of some variations of the canonical model on the system's behaviour [20].

Several discrete versions of Vicsek's self-propelled particles were developed by Deutsch *et al.* on a square lattice [21, 22] as well as Csahók and Vicsek on an hexagonal lattice [23]. Indeed, discrete dynamical systems such as lattice-gas cellular automata (LGCA) are well-suited tools for simulating complex systems with minimal computational cost because of their parallel, spatially-extended structure [24]. In spite of the discretisation, these models show a conservation of the swarm instability transition [25], whereas the resulting dynamics shows the appearance of novel behaviours [26]. Our objective here is to assess the robustness of the behaviour, by studying the dependence of Deutsch's model [22] on the definition of the system's lattice.

The swarming model comes with an unusual difficulty: we will show that because the updating rule being stochastic and reversible makes the system *ergodic*. This means that, if we consider the Markovian representation of the

system evolution, it will follow a random walk over the entire space of possible configurations. How can we then extract information about the dynamics in such an unstable environment? In fact, even though no configuration remains indefinitely stable, we will see that the system is subject to *metastability* [27], that is, it "can persist for a long period of time in a phase which is not the one favored by the thermodynamic parameters" [28]. In other words, once randomly initialised, the system will quickly converge towards some specific type of configurations, or *pattern*, and hold it for long times until random fluctuations allow it to escape this pattern for another one. These patterns act as "basins of attraction" which can thus be used to study the behaviour, by observing how the system organises in long times and for a large number of simulations.

In order to study the dynamics of the system, we propose the following method: after presenting a precise formal description of the model (Sec. 1), we start by determining the different patterns of the system by constraining the state space (Sec. 2), after which we quantify their stability, by studying the influence of an increasing spatial size (Sec. 3). We then reveal how the observation of the behaviour is influenced by resonance effects for any finite lattice (Sec. 4). Finally, we provide insights on how to observe the behaviour freely from lattice biases (Sec. 5), and finish by discussing the implications of our approach from the biological point of view (Sec. 6).

1 Deutsch lattice-gas model of swarming

1.1 Lattice-Gas Cellular Automata

A lattice-gas cellular automaton (LGCA) is a discrete dynamical system defined by a triplet $\{\mathcal{L}, \mathcal{N}, f_I\}$ where :

- $\mathcal{L} \subset \mathbb{Z}^2$ is the array that forms the cellular space.
- $\mathcal{N}$ is a finite set of vectors called the *neighbourhood*. It associates to a cell the set of its neighbouring cells. The sets $\mathcal{N}$ and $\mathcal{L}$ are such that for all $c \in \mathcal{L}$ and for all $n \in \mathcal{N}$, the *neighbour* $c + n$ is in $\mathcal{L}$.
- f_I is the *local interaction rule*.

In lattice-gas cellular automata, neighbouring cells are connected via *channels* through which *particles* can travel from one cell to another. For the sake of simplicity, we will consider here that each channel is associated to a neighbour. Consequently, the number of channels is given by $\nu = \text{card}(\mathcal{N})$.

A *configuration* $\boldsymbol{x}$ denotes the state of the automaton; it is defined as a function $\boldsymbol{x} : \mathcal{L} \to \mathcal{Q} \subset \mathbb{N}^\nu$ which maps each cell to a set of states for the channels. Each channel contains a given number of particles represented by an element of $\mathbb{N}$. The state of a cell $c \in \mathcal{L}$ is denoted by $\boldsymbol{x}_c = (x_1(c), ..., x_\nu(c)) \in \mathcal{Q}$, where $x_i(c) \in \mathbb{N}$ is the state of the i-th channel that connects cell c and its neighbour

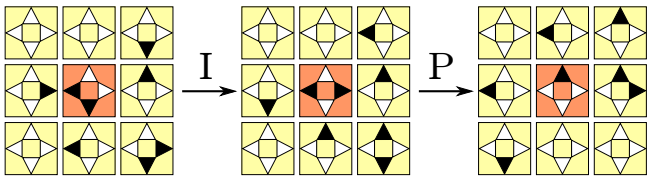

Figure 1: The cycle of a LGCA cell (a) at initial state, (b) after interaction step I, (c) after propagation step P. By convention, black and white triangles represent occupied and empty channels respectively.

$c + n_i$, with $\mathcal{N} = \{n_1, \ldots, n_\nu\}$.

The dynamics of a LGCA arises from the successive applications of two transitions applied to all cells synchronously (see example on Fig. 1):

- The *interaction step* I reorganises the particles within each cell.
  The result of the local transition $f_I : \mathcal{Q}^{\nu+1} \to \mathcal{Q}$ is denoted by:

$$\boldsymbol{x}_c^I = f_I(\boldsymbol{x}_c, \boldsymbol{x}_{c+n_1}, \ldots, \boldsymbol{x}_{c+n_\nu}), \text{ with } \mathcal{N} = \{n_1, \ldots, n_\nu\}. \tag{1}$$

- The *propagation step* P relocates all particles simultaneously in the same channel of the corresponding neighbour in $\mathcal{N}$.
  The result of the local transition $f_P : \mathcal{Q}^{\nu+1} \to \mathcal{Q}$ is given by:

$$\begin{aligned} \boldsymbol{x}_c^P &= f_P(\boldsymbol{x}_c^I, \boldsymbol{x}_{c+n_1}^I, \ldots, \boldsymbol{x}_{c+n_\nu}^I) \\ &= \left(x_1^I(c-n_1), \ldots, x_\nu^I(c-n_\nu)\right) \end{aligned} \tag{2}$$

The evolution of the system from a time t to the following time $t+1$ is determined by: $\boldsymbol{x}^{t+1} = P \circ I(\boldsymbol{x}^t)$. In this paper, initial configurations $\boldsymbol{x}^0$ are generated from a uniform distribution of *density* ρ, where ρ is the probability for *each channel*, independently, to contain a particle.

1.2 Swarm in Lattice-Gas Cellular Automata

The swarm model we study is taken from the work of Deutsch *et al.* compiled in a dedicated book (see [22], chapter 8.2). It describes a probabilistic *swarming interaction* rule in which a cell reorganises its particles according to a probability distribution that maximises local alignment.

This transition is particle-conserving and uses its neighbourhood state as a director field to align the cell particles. In this paper, the neighbourhood is composed of the vectors of the 4 nearest cells: $\mathcal{N} = \{(1,0),(0,1),(-1,0),(0,-1)\}$. Moreover, an *exclusion principle* is imposed: a channel contains at most one particle. As a consequence, a configuration is a vector $\boldsymbol{x} \in \mathcal{Q}^{\mathcal{L}}$ where the state for a cell c is a vector $\boldsymbol{x}_c \in \mathcal{Q} = \{0,1\}^4$.

To maximise the alignment of particles within cells, the computation of the individual rule uses two parameters:

(a) The *local flux* $\boldsymbol{J}_c(\boldsymbol{x})$ denotes the resulting particle direction in a cell c:

$$\boldsymbol{J}_c(\boldsymbol{x}) = \sum_{i=1}^{\nu} x_i(c) \cdot n_i \tag{3}$$

(b) The *director field* $\boldsymbol{D}_c(\boldsymbol{x})$ denotes the total flux of the neighbourhood of a cell c:

$$\boldsymbol{D}_c(\boldsymbol{x}) = \sum_{i=1}^{\nu} \boldsymbol{J}_{c+n_i}(\boldsymbol{x}) \tag{4}$$

Let $k(\boldsymbol{x}, c) = \sum_{i=1}^{\nu} x_i(c)$ be the the number of particles in a cell, and $\Omega(k) \subset \mathcal{Q}$ the possible states of a cell that contains k particles. For a cell $c \in \mathcal{L}$, the transition probability for the interaction step to update from a state $\boldsymbol{x}_c$ to a new state $\boldsymbol{x}_c^I \in \Omega(k(x, c))$ in the presence of the director field $\boldsymbol{D}_c(\boldsymbol{x})$ is given by:

$$P(\boldsymbol{x_c} \to \boldsymbol{x}_c^I) = \frac{1}{Z} \exp\Big[\alpha . \boldsymbol{J}_c(\boldsymbol{x}^I) \cdot \boldsymbol{D}_c(\boldsymbol{x})\Big] \tag{5}$$

where:

- The normalisation factor Z is such that $\sum_{\boldsymbol{x}_c^I \in \Omega(k(x,c))} P(\boldsymbol{x}_c \to \boldsymbol{x}_c^I) = 1$.
- The *alignment sensitivity* α is the control parameter controlling the intensity of the swarming effects.

With only the parameter α to control the behaviour continuously from random direction to deterministic alignment[1], the model is fairly simple and thus easy to explore. An example of a local application of the rule is shown on Fig. 2.

1.3 Reversibility and recurrence of behaviours

An important property of the update rule is that it is *reversible*, that is, for a given transition $\boldsymbol{x}^t \to \boldsymbol{x}^{t+1} \to \boldsymbol{x}^{t+2}$, the probability that $\boldsymbol{x}^{t+2} = \boldsymbol{x}^t$ (up to an interaction) is strictly positive (see example in Fig. 3). The direct result of this property is that if we consider the representation of all possible trajectories from an initial configuration, *i.e.* the system's *Markov chain*, it is *recurrent*, that is, it is always possible to go back to previously visited configurations. This means that once the initial state is determined, any reachable configuration will be visited an infinite number of times over infinite simulation times. As a consequence, the behaviour consists strictly speaking of a random walk over the entire space of reachable configurations, and studying behaviours can thus be challenging.

[1] When $\alpha = 0$, all outcomes $\boldsymbol{x}^I$ that conserve the number of particles have an equal probability to be selected, making the interaction step completely random. Inversely, when $\alpha \to \infty$, the system becomes pseudo-deterministic, that is, the selection almost always picks one of the configurations that maximises the local alignment.

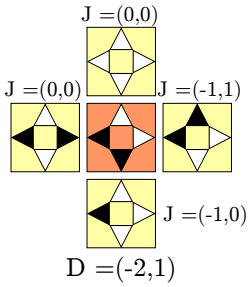

α	e^{α}	$e^{3\alpha}$	$e^{-\alpha}$	$e^{-3\alpha}$	e^{0}	e^{0}
0.5	1.65	4.48	0.06	0.02	1	1
1.5	4.48	90	0.02	0.01	1	1
4	54.6	10^{5}	0.01	10^{-6}	1	1

Figure 2: Example of the application of the swarm interaction rule for the central cell. Left: typical states for a cell and its neighbours, with neighbouring fluxes (Eq. 3) and the director field $\boldsymbol{D}_c(\boldsymbol{x})$ of the center cell (Eq. 4). Right: elements of $\Omega(2)$ along with a table of the computed weights (Eq. 5) for different values of α before normalisation to probability 1.

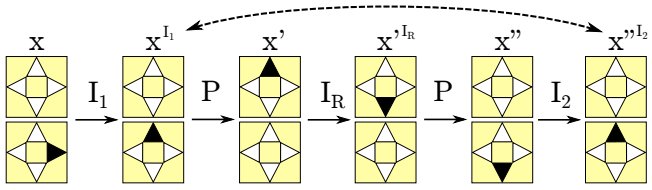

Figure 3: The proof of the reversibility of transitions applied to one particle. For any interaction I_1, and the interaction I_{R} that reverses channels within a cell, the configuration $\boldsymbol{x}''$ is equal to $\boldsymbol{x}$ up to an interaction, meaning that there exists I_2 so that $\boldsymbol{x}''^{I_2} = \boldsymbol{x}^{I_1}$.

However, previous observations of the behaviour revealed the emergence of *order* for particular values of the sensitivity α and the density ρ [10]. This implies that configurations have different energies, and that there must exist attractors which will appear more often from random configurations (attractivity) or remain present for longer simulation times (stability). These sets of ordered and stable configurations, referred to as *patterns*, can be used to characterise the behaviour of the system. The next section is devoted to a thorough search for these patterns.

2 Observation and identification of patterns

In the literature, analytical approaches have extensively described the organisation phenomenon occurring in this model [10]. However an experimental approach to the organisation process has to our knowledge never been studied. As a first step, we propose to identify the patterns by considering small lattices. Indeed, a small state space allows for a quicker exploration of the behaviour, and decreases the "distance" between patterns in terms of fluctuations, making it easier to make different patterns appear.

2.1 Monitoring the behaviour

How to characterise qualitatively the different patterns? We propose two tools to classify configurations: a visual method and a quantitative method.

Visual method Three types of *visualisations* are used:

- The *density visualisation* (Fig. 4 -Left) displays how many particles are in a cell. Empty cells are white, cells with 1, 2 and 3 particles are light, medium or dark gray, respectively, and fully occupied cells with 4 particles are black.
- The *flux visualisation*(Fig. 4 -Middle) is a new representation that we introduce in order to facilitate the reading of the resulting particles direction within cells by associating a color for each cell flux. A zero-flux cell is represented in white, while other types of flux show a different color for each corresponding cardinal point: N (green), N-E (lime), E (yellow), S-E (orange), S (red), S-W (magenta), W (blue), N-W (cyan).
- The *channel visualisation* (Fig. 4 -Right) displays the state of channels within cells by showing an oriented full triangle when a particle is present in a channel.

Quantitative method Two *order parameters* are used to quantify the behaviour:

- The *mean velocity* $\overline{\phi}$, introduced by Bussemaker *et al.*, averages horizontal and vertical momentum, in order to quantify a consensus in the direction of particles. For a configuration $\boldsymbol{x}$, it is defined by:

$$\overline{\phi}(\boldsymbol{x}) = \frac{1}{\mathrm{card}(\mathcal{L})} \left\| \sum_{c \in \mathcal{L}} J_c(\boldsymbol{x}) \right\|_\infty \quad \text{where } \|\boldsymbol{v}\|_\infty = |v_x| + |v_y|. \tag{6}$$

- To this parameter, we add the *mean alignment* $\overline{\gamma}$ to express whether particles are in average aligned with the flux of its neighbour:

$$\overline{\gamma}(\boldsymbol{x}) = \frac{1}{k(\boldsymbol{x})} \sum_{c \in \mathcal{L}} \frac{1}{\mathrm{card}(\mathcal{N})} J_c(\boldsymbol{x}) \cdot D_c(\boldsymbol{x}) \tag{7}$$

  where $k(\boldsymbol{x}) = \sum_{c \in \mathcal{L}} k(\boldsymbol{x}, c)$ is the total number of particles. Its value varies in $[-1, 1]$: $\overline{\gamma} = 1$ indicates that all particles are aligned, and for $\overline{\gamma} = -1$, all particles are antialigned[2].

These two parameters are complementary as they capture two distinct aspects of the spatial organisation of particles: the mean alignment $\overline{\gamma}$ monitors whether particles are on average aligned or antialigned with the neighbouring fluxes, while $\overline{\phi}$ captures a global consensus in directions.

2.2 Experimental protocol and observations

Throughout the paper, the following protocol will be used to assess the resulting behaviour for each given setting (α, ρ):

1. fix the lattice dimensions L and the parameters ρ and α,
2. start from an initial configuration, randomly generated by a Bernoulli distribution where each channel has a probability ρ to contain a particle, and $1 - \rho$ to be empty,
3. iterate the system for a fixed *transition time* T_{tr},
4. average the value of the parameters for a *sampling time* T_{sa} (optional),
5. use visualisations and order parameters to classify the configuration,
6. repeat from step 2 several times.

2.3 Identification of observed behaviour

We already know from the literature that the model displays a phase transition separating a chaotic disorganised phase from an organised phase for critical values of the parameters (α, ρ) [25]. The disorganised phase is therefore defined as follows:

[2]We borrow this term from spins systems in particle physics. Antialignment refers to the relationship between two particles whose directions are on the same axis, but in opposition.

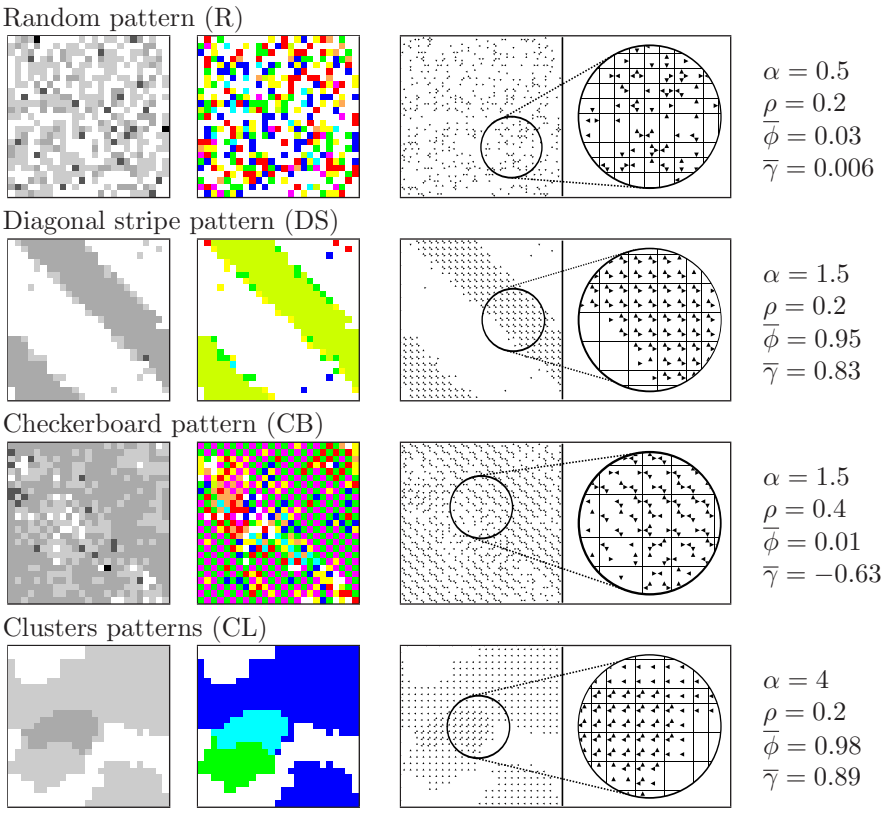

Figure 4: (color online) Major patterns, with associated visualisations and typical values for parameters. Configurations are obtained from random initial configuration, for $L = 25,\ t = 1000$.

Random Pattern (R). This category includes all configurations that do not display any observable ordered phenomenon. It is characterized by a zero-velocity and a zero-alignment and corresponds to the parametrical region of low sensitivity α and low particle density ρ.

The formation of patterns can be identified by the appearance of order, as captured by the parameters $\overline{\gamma}$ and $\overline{\phi}$. We now present the results of our exploration, divided between *major* and *minor* so as to reflect their attractivity.

Major patterns These patterns, listed in Fig. 4, are spatial organisations of particles which, for given input parameters[3], appear most often:

Diagonal stripe pattern (DS). By increasing progressively the values of (ρ, α), the behaviour suddenly switches and organises into a diagonal stripe that

[3]The system is strictly symmetrical around $\rho = 0.5$, by reversing `0`s and `1`s in the channels.

loops spatially over the periodic boundaries of the lattice. This pattern is composed of cells containing two particles, which all point to two orthogonal directions, and travels diagonally through the lattice in the combined directions of the particles. It is quantitatively characterised by high values for both mean velocity $\overline{\phi}$ and mean alignment $\overline{\gamma}$.

Checkerboard pattern (CB). For high values of the density ($\rho \in [0.3, 0.5]$), the system surprisingly organises into regions where each cell contains two particles that are antialigned with the neighbours' fluxes. This observation is confirmed by a zero-velocity $\overline{\phi}$ and a *negative* mean alignment $\overline{\gamma}$. We call this pattern "checkerboard" as the observation with the flux visualisation displays patterns of alternating "opposite colors", closely resembling the visualisation of antiferromagnetic ordering of a square Ising model.

Clusters pattern (CL). When the sensitivity increases drastically ($\alpha > 2$), the system no longer organises into a diagonal stripe, but into a small number of clusters of collinear particles. These clusters travel through the lattice and meet by overlapping occasionally, but remaining seemingly stable in the long run. It is characterised by a high mean alignment $\overline{\gamma}$ while the mean velocity $\overline{\phi}$ can take any value in $[0, 1]$.

Minor patterns These patterns, listed in Fig. 5, tend to appear less often, especially for large lattices:

Hybrid pattern (H). This pattern appears to be an hybrid between clusters and checkerboards: in one direction, particles are aligned with their neighbours, but for the orthogonal direction they are antialigned. Consequently, this pattern can be quantified by a near-zero mean alignment $\overline{\gamma}$ and a mean velocity $\overline{\phi} \sim 0.5$.

Belt pattern (B). This pattern appears as a single vertical or horizontal stripe (sometimes both), where particles are all antialigned. It is characterised by a negative mean alignment $\overline{\gamma}$ and a near-zero mean velocity $\overline{\phi}$.

Snake pattern (S). Particles organise in a diagonal stripe composed of particles which are oriented orthogonally to the neighbouring particles. This means that the mean alignment $\overline{\gamma}$ is zero, and the mean velocity $\overline{\phi}$ is positive.

These first observations show us that the behaviour is richer than the sole organisation phenomenon: while most majors patterns echo back to previous observations [22, 26], the checkerboard as well as the minors patterns constitute a novel observation for this model. For given input parameters (ρ, α), the system will repeatedly disorganise and organise into different patterns, each with different stability and attractivity. The measure and even the observation of stability through simulation can be problematic, as it involves long and highly-variable times. In order to estimate the system behaviour and study its robustness, we must thus consider each pattern in terms of attractivity, by relaxing the constraints on the lattice size to exclude related effects.

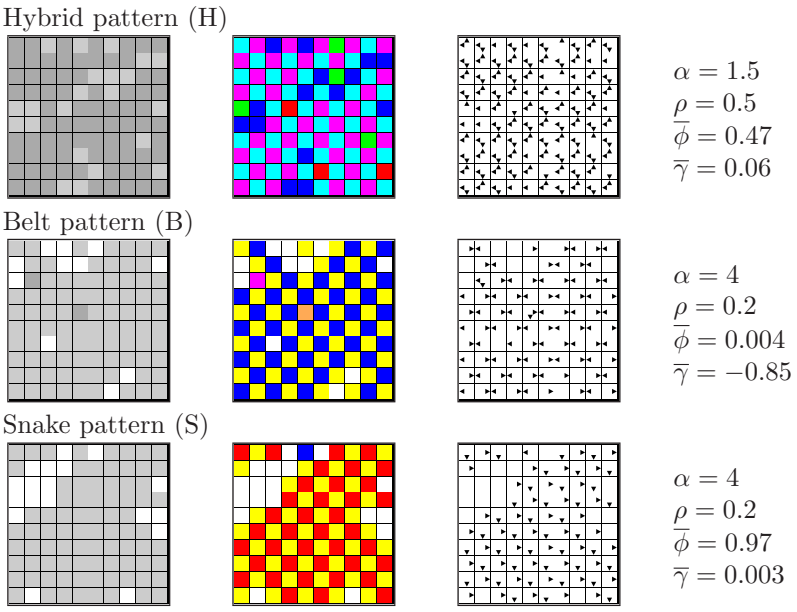

Figure 5: (color online) Minor patterns, with associated visualisations and typical values of parameters. Configurations are obtained from random initial configuration, for $L = 10,\ t = 1000$.

3 Attractivity and lattice scale

We now try to organise patterns in the parameter space of the density ρ, the sensitivity α and the lattice size L. In particular, we want to determine which parameters have an influence on the attractivity of patterns, that is, how often it will appear from a random initial configuration after a long simulation time.

3.1 Scale-dependence of minor patterns

A first step in assessing whether the observed patterns are independent from the size of the lattice consists in ruling out those which stability changes with the size of the lattice L. To do so, we propose to carry out simulations for increasing lattice sizes ($L = 10, 20, 40$) and different input parameters, by iterating the system an arbitrary number of step and observing the resulting behaviour. As seen on Fig. 6, the output shows that minor patterns become less attractive as the size of the lattice increases[4]. Minor patterns therefore appear connected to small lattices, which can be considered a bias of the model determination on the system's behaviour. We determine experimentally that simulations require a reasonably large lattice (here $L > 50$) in order to avoid the appearance of this

[4]Note that on some specific cases, major patterns appear less often when conflicting with another major pattern, such as the diagonal stripe in Fig. 6-Right.

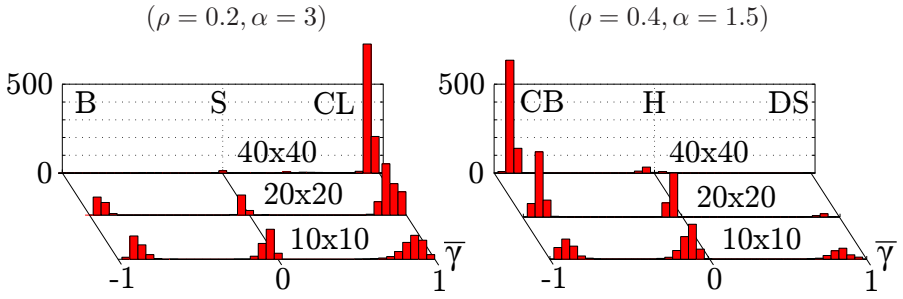

Figure 6: Distribution of mean alignment $\overline{\gamma}$ for different lattice sizes. Above each peak is specified the corresponding identified pattern. Samples are made of 1000 configurations obtained for $(T_{\rm tr} = 10^5, T_{\rm sa} = 100)$.

type of small-size effects.

3.2 Distribution of major patterns in the parametrical plane

By contrast, increasing the lattice scale has limited effects on the aspect and evolution of the major patterns. First, it becomes harder for particles to organise in a single global pattern as space widens. Instead, we observe several patterns that appear locally and co-exist for some time, until they all merge into a unique pattern :

- In the case of the diagonal stripe, several stripes of conflicting directions may appear simultaneously, until only one direction remains.
- The checkerboard pattern first appears scattered in several "regions" of local checkerboards of different directions (*e.g.* NW/SE versus NE/SW), until a unified checkerboard covers the entire lattice.

It is interesting to note that for each given set of parameters (ρ, α), only one type of pattern appears preponderantly. The corresponding parametrical regions for each major patterns are displayed on Fig. 7. In particular, it is experimentally impossible to observe more than one type of pattern anywhere *inside* these regions whereas inbetween settings (dashed lines) easily display pattern shifts and the occasional coexistence of several patterns of different types.

Our observations suggests that the three major patterns remain stable for large lattices, for long enough simulations times. However, the question remains as to whether this observation of the behaviour can be generalised for *any* lattice $\mathcal{L}$.

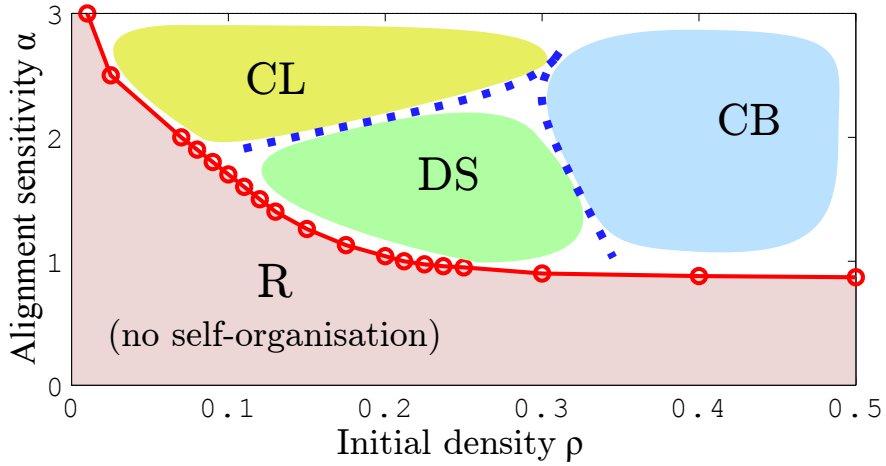

Figure 7: Spatial distribution of the disordered and ordered phases in the density-sensitivity parametric plane. We divided the ordered phase into approximated regions of appearance for each observed patterns. The circles represent experimental observations of the phase transition.

4 Influence of the lattice size ratio

In its first definition, the diagonal stripe is presented as a cluster of particles looping over the periodic boundaries of a *square* lattice. One may then wonder what happens when the lattice has unequal dimensions. This time, we take a rectangular lattice $\mathcal{L} = (\mathbb{Z}/L_x\mathbb{Z}) \times (\mathbb{Z}/L_y\mathbb{Z})$, where L_x and L_y are respectively the width and height of the lattice. For $\rho = 0.2$, $\alpha = 1.5$ and different ratios of L_x and L_y, the system still organises into a diagonal stripe, but the observation is somewhat different. Several cases can be distinguished (see Fig. 8-Left):

- Harmonic or quasi-harmonic ratios (*e.g.* 50×100, 33×100) show a diagonal stripe pattern that loops one or several times over the periodic boundaries.
- For other "more complex" ratios (*e.g.* 66×100), the configuration displays an unfinished, distorted diagonal stripe, as it can no longer loop "regularly" over the periodic boundaries. Over very long simulation times, the system might finally find a stable pattern (see 66×100 (b)).

Note that the clusters and checkerboards patterns remain both unchanged. From these observations, we conclude that the regularity of the lattice influences the behaviour of the system, by disturbing the stability of the diagonal stripe pattern. To quantify this phenomenon, we propose to compare the transitions for different lattice ratios. Consider the following process: starting from a fixed density $\rho = 0.2$ and given lattice dimensions (L_x, L_y), we measure the mean alignment $\overline{\gamma}$ after a few thousands steps for different values of the sensitivity α. We thus obtain a plot of $\overline{\gamma}$ versus α, displayed in Fig. 8-Right.

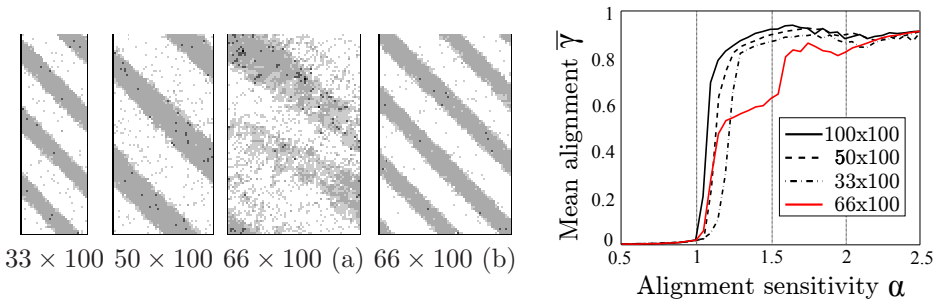

Figure 8: Left: typical configurations obtained for different lattice ratios after 1000 time steps ; note that the case 66×100 is shown at two different times: at $t = 1000$ (a) and at $t = 10^6$ (b). Right: a quanfitication of the corresponding transitions, as plot of the mean alignment $\overline{\gamma}$ versus the alignement sensitivity α, for different lattice ratios with $(T_{\text{tr}} = 10^5, T_{\text{sa}} = 100)$.

It is interesting to note that although the transition between the disordered and the ordered phases is always observed, the profile of the transition as well as the critical point (ρ, α_c) slightly change with the considered ratio. These observations support the hypothesis of a strong connection between the formation of the diagonal stripe pattern and the regularity of the lattice. A possible explanation stands as follows: the diagonal stripe pattern emerges from the periodic interactions of diagonal clusters, which by crossing regularly, compete and grow until a consensual configuration is found. Changing the ratio thus changes the regularity of these encounters and perturbates the stability of the diagonal stripe pattern. Our interpretation of this phenomenon is that it can be considered as a "resonance" effect caused by the finite lattice with periodic boundaries.

More generally, this means that a finite implementation of the model induces a bias in the behaviour of the system. Now this statement questions our understanding of the dynamics: how much of the resonance effects tamper with the resulting behaviour? To tackle this issue, we propose to consider the case of an infinite lattice $\mathcal{L} = \mathbb{Z}^2$ and compare the observed behaviour with the finite case.

5 Overcoming the resonance effects

Changing the implementation of the model from a finite to an infinite lattice suggests drastic changes in hypotheses. If the number of possible configurations is infinite, the probability to escape a given pattern through fluctuations becomes zero, and the behaviour can no longer be considered as metastable. Instead, we will observe the emergence of phases, that is, local behaviours that occur statistically everywhere on the lattice and remain stable.

In order to study the behaviour without long-term resonance effects, we pro-

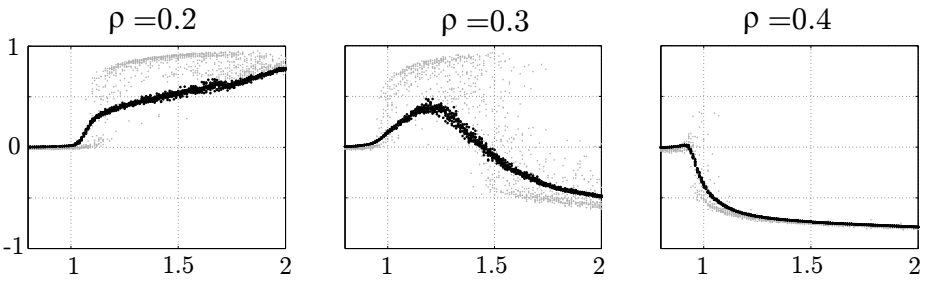

Figure 9: The organisation phenomena for different values of α at fixed ρ. Dots represent independent sampling for $(T_{\text{tr}} = 1400, T_{\text{sa}} = 100)$ and for different lattice settings – black accounts for $L = 1500$, and gray for $L = 100$.

pose to choose coherent values for the space and time dimensions of the simulations. This means that to estimate the behaviour in a given order of T, we need to use an equivalent size $L \approx T$ for the lattice. Similarly, to study the asymptotic behaviour, both dimensions must increase simultaneously when passing to the limit. As an example, we computed samples of lattice sizes $L = 1500$ and $L = 100$ respectively for $(T_{\text{tr}} = 1400, T_{\text{sa}} = 100)$. As observed in Fig. 9, the difference in the resulting behaviours is significant, as captured by the evolution of order parameters versus the sensitivity α:

- The transition between the disorganised and organised phases greatly differs between experiments: for the case $L = 100$, the transition is sharp and almost immediate whereas for the case $L = 1500$, the transition is progressive.
- The plot for densities $\rho = 0.2$ and 0.4 confirms the existence of at least an "aligned" and an "antialigned" phase. The case $\rho = 0.3$ appears to show an intermediate case, but the precise transition is not visible.
- The differentiation between the diagonal stripe and the clusters pattern is *a priori* not apparent.

Our simulations are too limited to assess asymptotic behaviours, as their cost both in terms of time and memory reached computational limits. However, they are sufficient to display tendencies in the organisation of particles and reveal divergent behaviours. In particular, we conjecture from the observation of order parameters that the asymptotic behaviour of the system divides up in at least three phases: disorganised, aligned and antialigned. Moreover, a preliminary visual experiment using a $L = 500$ lattice and $t = 500$ suggests a visible differentiation of behaviour between the diagonal stripe and the clusters pattern (see Fig. 10). Determining whether there exists a distinct phase for the diagonal stripe pattern is an interesting problem left for future work.

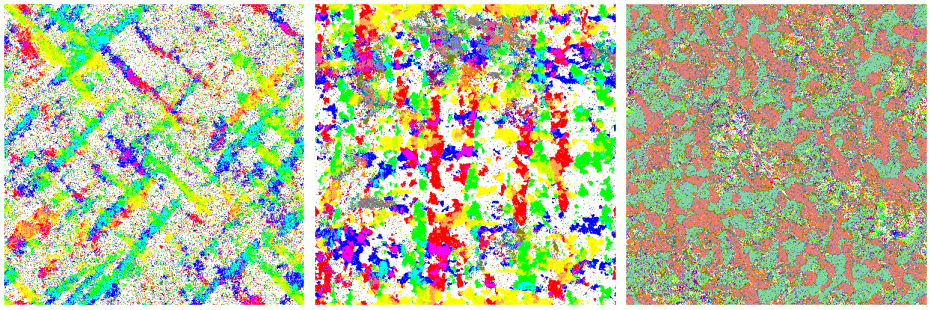

$\rho = 0.2, \alpha = 1.5$ Stripes | $\rho = 0.2, \alpha = 3$ Clusters | $\rho = 0.4, \alpha = 1.5$ Checkerboards

Figure 10: (color online) Flux visualisation of large-scale configurations for non-biased simulations, with equal space and time dimensions ($t = 500, L = 500$).

6 Conclusions and perspectives

In spite of the model following a stochastic updating rule controlled by the sole parameter α, and behaviours being derived from random initial configuration determined only by their density ρ, a surprisingly high number of distinctive patterns could be identified. By simulating the model for conditions that were not planned in its original design, we discovered that the organised phase could result in unexpected behaviours that exhibit the limits of the model.

For instance, the stability of antialigned patterns (*e.g.* checkerboards) are an important result of this study: although particles try to maximise their own alignment, the global alignment remains negative. A plausible hypothesis lies in that by "pushing" these parameters to extreme, non-realistic values, we reduce the "degrees of freedom" of cells and exacerbate certain aspects of the individual behaviour at the expense of other possibilities. Thus, saturating the lattice with particles has as an effect to enhance the discretisation effects of the lattice granularity. It is however undeniable that the checkerboard is intrinsically linked to the synchronous updating scheme of the model, as showed in a previous work [29], which questions its "realism" with regards to a biological context.

The nature of the phase transitions Our experiments echo back to an unresolved issue on the nature of the transitions in this model of swarming. The swarm instability, the transition between the disordered and the ordered phases, has been previously documented in numerous studies of lattice-gas models. For instance, Csahók *et al.*, reported experimentally a "weakly first-order", using a 6-direction version of the model [23], and Bussemaker *et al.* reckoned that it was second-order with a mean-field approach [25].

Our simulations suggest a drastically different observation of the phase transition due to resonance effects, depending on the scales of the time and space dimensions when passing to the limit. In other terms, it means that the limits

of time t and space L are non-commutative, that is, fixing L and studying the behaviour for $t \to \infty$ is not equivalent to fixing t and studying the behaviour for $L \to \infty$. According to our observation, this implies that the phase transition may appear first-order in the case of a finite lattice, but would actually be of higher-order in open space.

Modeling and studying robustness The goal of studying robustness is to try to understand behaviours through the quantification of changes for variations of the model attributes. Although we focused on the influence of the lattice definition in this paper, parallel studies report similar types of dependence, such as synchronous updating [29] or different individual rules [26].

The construction of simple models for natural phenomena, such as the model presented here, should take into account its robustness. Indeed, the simplification and discretisation of models may facilitate simulations, by reducing the size of the search space, but also increases the chance that the behaviour of the system depends on the model itself. If robustness study manages to exhibit those dependences, it is up to the designer to develop and use methods to study robustness, and determine which behaviours are relevant to the simulated phenomenon and which are simulation biases which should be avoided.

References

[1] A. Turing, The chemical basis of morphogenesis, Philosophical Transactions Of the Royal Society (London) 237 (1952) 5–72.

[2] G. B. Ermentrout, L. Edelstein-Keshet, Cellular automata approaches to biological modeling, Journal of Theoretical Biology 160 (1) (1993) 97–133.

[3] V. Chevrier, N. Fatès, How important are updating schemes in multi-agent systems? an illustration on a multi-turmite model, in: Proceedings of the 9th International Conference on Autonomous Agents and Multiagent Systems, 2010, pp. 533–540.

[4] J. Slotine, W. Li, et al., Applied nonlinear control, Vol. 66, Prentice hall Englewood Cliffs, New Jersey, 1991.

[5] O. Bouré, N. Fatès, V. Chevrier, Probing robustness of cellular automata through variations of asynchronous updating, Natural Computing *(Online First)* 11 (4) (2012) 553–564.

[6] C. Grilo, L. Correia, Effects of asynchronism on evolutionary games, Journal of Theoretical Biology 269 (1) (2011) 109–122.

[7] T. Vicsek, A. Zafeiris, Collective motion, Physics Reports 517 (3–4) (2012) 71 – 140.

[8] A. Deutsch, G. Theraulaz, T. Vicsek, Collective motion in biological systems, Interface Focus 2 (2012) 689–692.

[9] F. Peruani, F. Ginelli, M. Bär, H. Chaté, Polar vs. apolar alignment in systems of polar self-propelled particles, Journal of Physics: Conference Series 297 (1) (2011) 012014.

[10] A. Deutsch, Orientation-induced pattern formation: Swarm dynamics in a lattice-gas automaton model, International Journal of Bifurcation and Chaos 06 (09) (1996) 1735–1752.

[11] S. Whitelam, E. H. Feng, M. F. Hagan, P. L. Geissler, The role of collective motion in examples of coarsening and self-assembly, Soft Matter 5 (2009) 1251–1262.

[12] B. Chopard, R. Ouared, A. Deutsch, H. Hatzikirou, D. Wolf-Gladrow, Lattice-gas cellular automaton models for biology: From fluids to cells, Acta Biotheoretica 58 (2010) 329–340.

[13] H. Hatzikirou, L. Brusch, C. Schaller, M. Simon, A. Deutsch, Prediction of traveling front behavior in a lattice-gas cellular automaton model for tumor invasion, Computers Mathematics with Applications 59 (7) (2010) 2326–2339.

[14] D. Helbing, M. Isobe, T. Nagatani, K. Takimoto, Lattice gas simulation of experimentally studied evacuation dynamics, Physical Review E 67 (2003) 067101.

[15] A. Lerner, Y. Chrysanthou, D. Lischinski, Crowds by example, Computer Graphics Forum 26 (3) (2007) 655–664.

[16] J. Kennedy, R. C. Eberhart, A discrete binary version of the particle swarm algorithm, Systems, Man, and Cybernetics 5 (1997) 4104–4108.

[17] H. Leung, R. Kothari, A. A. Minai, Phase transition in a swarm algorithm for self-organized construction, Physical Review E 68 (4) (2003) 046111.

[18] T. Vicsek, A. Czirók, E. Ben-Jacob, I. Cohen, O. Sochet, Novel type of phase transition in a system of self-driven particles, Physical Review Letters 75 (1995) 1226.

[19] F. Peruani, A. Deutsch, M. Bär, A mean-field theory for self-propelled particles interacting by velocity alignment mechanisms, The European Physical Journal - Special Topics 157 (2008) 111–122.

[20] H. Chaté, F. Ginelli, G. Grégoire, F. Peruani, F. Raynaud, Modeling collective motion: variations on the Vicsek model, The European Physical Journal B - Condensed Matter and Complex Systems 64 (2008) 451–456, 10.1140/epjb/e2008-00275-9.

[21] A. Deutsch, Orientation-induced pattern formation: swarm dynamics in a lattice-gas automaton model, International Journal of Bifurcation and Chaos 6 (1996) 1735–1752.

[22] A. Deutsch, S. Dormann, Cellular Automaton Modeling of Biological Pattern Formation, Birkhauser Boston, 2005.

[23] Z. Csahók, T. Vicsek, Lattice-gas model for collective biological motion, Physical Review E 52 (1998) 5297–5303.

[24] C. Mente, I. Prade, L. Brusch, G. Breier, A. Deutsch, Parameter estimation with a novel gradient-based optimization method for biological lattice-gas cellular automaton models, Journal of Mathematical Biology 63 (2011) 173–200.

[25] H. J. Bussemaker, A. Deutsch, E. Geigant, Mean-field analysis of a dynamical phase transition in a cellular automaton model for collective motion, Physical Review Letters 78 (26) (1997) 5018–5021.

[26] F. Peruani, T. Klauss, A. Deutsch, A. Voss-Boehme, Traffic jams, gliders, and bands in the quest for collective motion of self-propelled particles, Physical Review Letters 106 (2011) 128101.

[27] F. Manzo, E. Olivieri, F. Nardi, E. Scoppola, On the essential features of metastability: Tunnelling time and critical configurations, Journal of Statistical Physics 115 (2004) 591–642.

[28] E. Cirillo, F. Nardi, C. Spitoni, Metastability for reversible probabilistic cellular automata with self-interaction, Journal of Statistical Physics 132 (2008) 431–471.

[29] O. Bouré, N. Fatès, V. Chevrier, First steps on asynchronous lattice-gas models with an application to a swarming rule, in: G. C. Sirakoulis, S. Bandini (Eds.), Cellular Automata, Vol. 7495 of Lecture Notes in Computer Science, Springer, 2012, pp. 633–642.